A Multistatic Uniform Diffraction Tomographic Algorithm for Real-Time Moisture Detection

Adel Omrani*, Guido Link*, John Jelonnek*^
institute for Pulsed Power and Microwave Technology (IHM)
t Institute of Radio Frequency Engineering and Electronics (IHE)
Karlsruhe Institute of Technology, Karlsruhe, Germany
Email: adel.hamzekalaei@kit.edu

***Abstract*— To obtain the moisture distribution inside a polymer foam after drying in a conveyor belt system in real time, a Multistatic Uniform Diffraction Tomography (MUDT) imaging algorithm is proposed. It is estimated that MUDT provides a better spatial resolution than the original uniform diffraction tomography (UDT). Additionally, it allows to resolve the distribution of the different scatterers, which is shown by simulation result.**

***Index Terms*— microwave imaging, tomography, moisture detection**

I. Introduction

Microwave drying is an emerging technology of increasing interest. It is the preferred method of choice particularly for polymer foam that has low thermal conductivity. Using an intelligent control of distributed microwave sources [1], non-uniform moisture distribution could be much more efficiently addressed. But, it requires the in-situ and non-invasive measurements of the unknown moisture distribution inside the material under test. A novel method for microwave tomography (MWT) in real time is in preparation for moisture detection of a polymer foam that will be used in combination with a HEPHAISTOS microwave system, as shown in Fig. 1a.

This HEPHAISTOS microwave oven has a patented hexagonal cross-section [2]. In our specific case, the overall length and hexagon circumferential diameters of the oven are 4 m and 1 m, respectively. The oven has a modular structure and consists of three microwave modules of the same type, each 1 m in length and with six slotted waveguide antennas mounted. Each of those antennas is fed by a 2 kW magnetron working at the 2.45 GHz ISM frequency band. The total microwave power installed in the system is about 36 kW. In addition, a 28 kW convective heating system is installed to help the removal of the water vapor out of the microwave-drying chamber. That avoids the condensing of water on the cold metal walls of the microwave oven. Another unique feature of the HEPHAISTOS system is the conveyor belt as shown in Fig. 1, which allows a continuous production process [3].

In [4] a Through Wall Imaging (TWI) method is proposed that bases on the Uniform Diffraction Tomography (UDT) method. The location of an object inside or behind the wall is determined by the linear relationship between the object function and the received signal in the spectral domain for the multilayered media. Using a conveyor belt system complicates the task to locate an object significantly. Not only the real-time image reconstruction is important but also the real-time data acquisition is a critical task. Using only one antenna and moving the antenna for data acquisition is not applicable in fast data acquisition so the array of the antennas needs to be fixed. On the other side, the number of antennas cannot be too high because, again, it takes time for data collection. Under those conditions, i.e., 1) the low number of antennas, and, 2) if two adjacent antennas are not in close vicinity to each other, the UDT imaging algorithm fails to truly reconstruct the location of the scatterers. The MUDT proposed here does overcome this problem. It provides high-resolution and real-time images through the foam by the same number of transmitters and employing non-diagonal elements of the scattering matrix. For simplicity, the algorithm is presented for a 2-D problem. The paper is organized as follows: in Section II the MUDT formulation and differences with UDT are presented. In section III the simulation results are presented. Concluding remarks are provided in section IV.

Fig. 1. Microwave drying system with conveyor-belt.

II. MULTISTATIC UNIFORM DIFFRACTION TOMOGRAPHY

A. The Forward Model

The 2-D configuration of the multistatic microwave imaging system is illustrated in Fig. 2. The array of antennas is located in semi-infinite free space and above the polymer foam with

variations of dielectric properties in the ^-direction only. The distance of the antenna from the top of the polymer foam is t_1. t_2 is the thickness of the polymer foam with the permittivity £2.

The Lippmann-Schwinger integral equation of the EM scattering problem shown in Fig. 2, can be written in the following form [5], [6]:

$$E s\backslash r_r, n) = E\text{“}\ (V_r, f) \text{—} E\ mc(r_r, n) = k_2 \int_n dr' G(n_1\backslash r_r, f) \bullet O(f,) Ef\ t(f') \quad (1)$$

where EJ^ is the total electric field in layer n (n = 1, 2, 3), Esct represents the scattered field due to the unknown irregularities in layer n, while Einc denotes the incident electric field. $O(r') = (e(f') \text{—} e_b)$ is the object function. $e(f')$ is the profile of the permittivity of the target and e_b denotes the permittivity of the background. Here, a time harmonic field is assumed. Hence, the complex time harmonic function e^{-j^t} can be eliminated from the equation. w is the angular frequency. In (1), the vectors $f_r = (y_r, z_r)$ and $f_t = (y_t, z_t)$ represent observation and source points while $G(n1)(r_r, r_t)$ is the background (multilayered media without any scatterer inside) dyadic Green's function (DGF). The superscript (n1) denotes that the source point is located in layer *1* and the observation point is in layer n.

Under the first-order Born approximation the total electric field Etot can be replaced by the background electric field of the layer and due to the excitation by a line source the electric field can be replaced by the Green's function and also using the symmetry property of Green's function. Equation *1* can be expressed as stated in [5], [7]

$$E\quad, f_t) = k2 \int_n dr' G(n_1 H f_r, f\ ) \bullet O(r,) G^{\backslash}(n1)(r,, r_r)(f/) \quad (2)$$

Furthermore, for writing the background Green's function in layer n, the contrast between the layers is assumed to be small and the reflected wave from the layers is suppressed. So, the Green's function is modeled by the incident field in that layer. If the contrast for the permittivity between the different layers is sufficiently large, this assumption leads to a late-time shadow image in the layer.

The spectral representation of the Green's function in the nth layer when the line source is located in region 1 is [6], [8]

$$G(n_1)(r, ft) \quad \frac{1}{n} \int_{-\infty}^{\infty} \frac{T_n(k_y, k_z) - e^{jk_{zn}(z - z_t)}}{k_{z1}} Ey(y - yt)\, dky \quad (3)$$

If $z > zt$ and $Q(kn \text{—} k^{)1/2} < 0$. $T(ky, kz)$ is the transmission coefficient in the nth layer and can be obtained by applying the boundary conditions between layers for the transverse magnetic field in x-direction (TM$) [6]. The dispersion relation in the layer l is expressed by $kzl = k_2 \text{—} k2l$ and

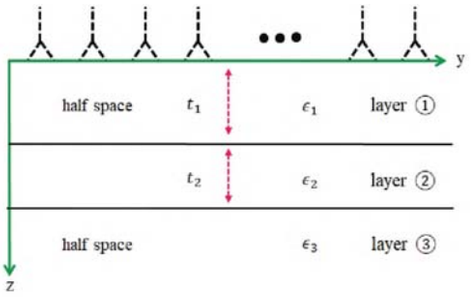

Fig. 2. The antenna array is located above a polymer foam. The first and last media are half space.

$ki = koi/el$ is the wavenumber in layer l while k_0 is the free-space wavenumber.

The above representation of the scattered field, allows to extend the UDT to the multistatic case (transmitter and receiver are not co-located) where the non-diagonal element of the scattering matrix can be employed for the image reconstruction which significantly increases the resolution as a consequence.

B. MUDT Inverse Scattering

From (2) the object function can be determined. Substituting (3) in (2) with the prime integrand for the second Green's term, changing variables to k" = $ky + k'y$ and using 2-D spatial Fourier definition for the received signal an inner integral is obtained. The stationary phase method can be applied to evaluate that inner integral asymptotically for $k0z$ as follows:

$$i k) \quad \int_{ky} \backslash T_n(f, kz^2 \backslash A_n(kyi z, w) \quad e^{j[k\backslash n_{zL} t\, nik'\backslash, \kappa Jn, tl) + (yt - y\, r) \sim f\ ]} \quad (4)$$

where $kzn = ^4kn \text{—} ky$ and

$$An(ky, z, w) = k2_{kzn} z + d_{dky}^{2} \wedge Trn]\backslash H_2^L \quad (5)$$

Where / denotes the phase and tl is the thickness of the layer l (l = *1*, 2). The term $(yt \text{—} yr)$ in the phase of the inner integral is the difference between UDT and MUDT which is the consequence of considering the problem multistatic rather than monostatic. In other words, if, in (4) the transmitter and receiver are located at the same place (monostatic measurement or $yt = yr$), the UDT formulation will be obtained [4]. However, the non-diagonal elements of the scattering matrix cannot be used in the inversion scheme and this is the source of the shadowing image and low resolution in the UDT compare to the MUDT.

After a straightforward simplification and using the Fourier transform definition, the object function for the MUDT can be obtained as follows

$$O_n(y,z)=\left|\frac{\int_\omega \int_{-\infty}^{\infty} \frac{1}{|\tilde{T}_n|^2}\frac{k_\eta}{\omega k_{zn}} e^{-j\left[k''_{zn}z+\angle\tilde{T}_n\left(\frac{k''_y}{2},k''_{zn},t_l\right)+(y_t-y_r)-\frac{\pi}{4}\right]}\tilde{E}^{sct}(k''_y,\omega)e^{jk_y y''}dk_y d\omega}{2\pi\int_\omega\int_{-\infty}^{\infty}\frac{k_\eta}{\omega k''_{zn}}\frac{1}{\sqrt{A_n(k''_y,z,\omega)}}dk_y d\omega}\right| \quad (6)$$

Where $E\,sct(k'',E)$ is the spatial Fourier transform of the received scattered filed, and

$$\int_{-TO}^{+ro} E\,sct(y_t,E)e^{-jk\,y_y t}dy_t. \quad (7)$$

III. MUDT SIMULATION RESULTS

The MUDT method is used to obtain the location of the unknown scatterers inside the polymer foam and it is used to compare the results with the UDT. The numerical scattered field is generated by the use of the time domain solver of the commercial Software CST Studio Suite® for a single layer of the foam and 7 x-band open-waveguide antennas for multistatic transmitting/receiving the signal as shown in Fig. 3. The distance between two adjacent antennae is 5cm. Following [9], an antenna de-embedding is performed to relate the scattering parameters (S-parameters) to the electric field for MUDT imaging. It is worth mentioning the permittivity correlates with a certain amount of the moisture (M_n) based on the wet basis, which is the percentage equivalent of the ratio of the weight of the water to the weight of the wet foam. Here, it is assumed that the permittivity of the scatterer is $\epsilon_r = 2$ which is equivalent to M_n & 40%. Moreover, additional to the diagonal elements of the scattering matrix (DT and UDT), the 5^ +!) ($i = 1, 2, \ldots, 6$) is also used in the MUDT for image reconstruction. Fig. 4(a) shows the reconstructed image with UDT and Fig, 4(b) shows the reconstructed image with MUDT. As can be seen from these two figures, with the MUDT method, a good resolution is obtained. Furthermore, the shadowing images with MUDT is significantly reduced compared to the UDT method.

IV. CONCLUSION

A multistatic uniform diffraction tomography is proposed to obtain the moisture distribution inside a polymer foam in a running belt system in a real-time fashion. MUDT overcomes low resolution caused by UDT, due to the monostatic nature of this method, by using the non-diagonal element of the scattering matrix rather than only the diagonal elements. The result shows a significant increase in the quality of the final image. In the next study, we obtain the moisture level inside the foam after reconstruction of the location of that by defining an error function and a certain calibration.

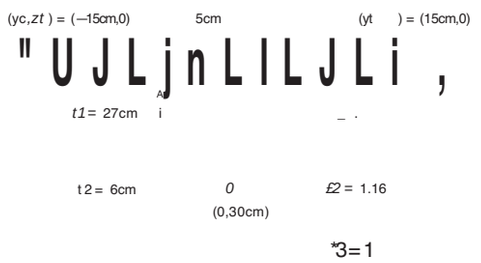

Fig. 3. 2-D simulated imaging scenario.

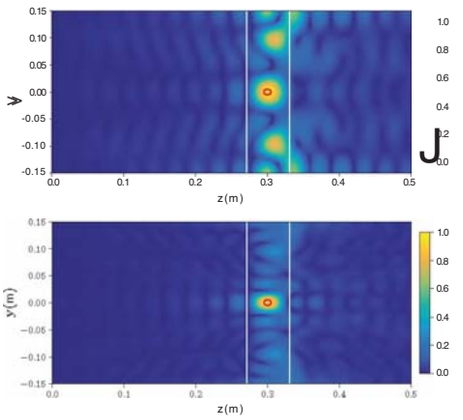

Fig. 4. Corresponding normalized (Top) UDT (Bottom) MUDT imaging results.

Acknowledgment

This project has received funding from the European Union's Horizon 2020 research and innovation program under the Marie Sklodowska-Curie grant agreement No. 764902.

References

[1] Y. Sun, "Adaptive and Intelligent Temperature Control of Microwave Heating Systems with Multiple Sources," PhD desertion, Karlsruhe Institute of Technology, 2014.

[2] L. Feher, G. Link, "Hochmodiger Mikrowellenresonator fur die hochtemperaturbehandlung von Werkstoffen,"DE19633245C1. Aug. 17, 1996.

[3] G. Link, et al, "Faserverbund-Leichtbau mit Automatisierter Mikrowellenprozesstechnik hoher Energieeffizienz (FLAME): Schlussbericht des BMBF-Verbundprojektes (KIT Scientific Reports;7701)," IHM Projects Information, Internet https://publikationen.bibliothek.kit.edu/1000047509.

[4] K. Ren and R. J. Burkholder, "A Uniform Diffraction Tomographic Imaging Algorithm for Near-Field Microwave Scanning Through Stratified Media," IEEE Trans. Antennas Propag., vol. 64, no. 12, pp. 5198-5207, Dec. 2016.

[5] C. T. Tai, "Dyadic Green Functions in Electromagnetic Theory," 2nd ed. NY, United Sates, 1994.

[6] W. C. Chew, "Waves and Fields in Inhomogeneous Media," New York, NY, USA: IEEE Press, 1995.

[7] A. Omrani, M. Moghadasi, M. Dehmollaian, Localisation and permittivity extraction of an embedded cylinder using decomposition of the time reversal operator," IET Microwaves, Antennas and Propag., vol. 14, no. 9, pp.851-859, July 2020.

[8] D. Dudley, "Mathematical foundations for electromagnetic theory." New York: IEEE press, 1994.

[9] S. Sadeghi, K. Mohammadpour-Aghdam, K. Ren, R. Faraji-Dana, and R. J. Burkholder, "A pole-extraction algorithm for wall characterization in through-the-wall imaging systems," IEEE Trans. Antennas Propag., vol. 67, no. 11, pp. 7106-7113, Nov. 2019.